

Nonlocal Andreev transport through an interacting quantum dot

David Futterer,¹ Michele Governale,¹ Marco G. Pala,² and Jürgen König^{1,3}

¹*Institut für Theoretische Physik III, Ruhr-Universität Bochum, D-44780 Bochum, Germany*

²*IMEP-LAHC-MINATEC (UMR CNRS/INPG/UJF 5130), 38016 Grenoble, France*

³*Theoretische Physik, Universität Duisburg-Essen, 47048 Duisburg, Germany*

(Received 14 November 2008; published 9 February 2009)

We investigate subgap transport through a single-level quantum dot tunnel coupled to one superconducting and two normal-conducting leads. Despite the tendency of a large charging energy to suppress the equilibrium proximity effect, a finite Andreev current through the dot can be achieved in nonequilibrium situations. We propose two schemes to identify nonlocal Andreev transport. In one of them, the presence of strong Coulomb interaction leads to negative values of the nonlocal conductance as a clear signal of nonlocal Andreev transport.

DOI: 10.1103/PhysRevB.79.054505

PACS number(s): 74.45.+c, 73.63.Kv, 73.21.La, 73.23.Hk

I. INTRODUCTION

The entanglement of electrons in Cooper pairs of a superconductor can generate nonlocal transport effects. A prominent example is *crossed Andreev reflection* (CAR) at the contact between a superconductor and two normal leads. There the two electrons with opposite spins and symmetric energies with respect to the Fermi level of the superconductor, that are transferred through the normal-superconductor interface via Andreev reflection,¹ originate from or end up in different normal leads. This is a nonlocal transport phenomenon which has been extensively studied both theoretically^{2–11} and experimentally.^{12–16}

The main problem to identify the nonlocality of CAR in a transport measurement is to separate it from other transport channels. In this paper, we study nonlocal Andreev transport through a single-level quantum dot. The quantum-dot level energy can be tuned by a gate voltage, which opens the possibility to control the Andreev transport channels. At first glance, strong Coulomb interaction in the quantum dot seems to be counterproductive: the formation of a finite equilibrium superconducting pair amplitude is suppressed since a large charging energy prevents the equilibrium state to be a coherent superposition of dot states with particle numbers differing by two and Cooper pairs can be transferred through the dot by higher-order tunneling processes (cotunneling) only. On the other hand, a finite *nonequilibrium* pair amplitude in the dot can be achieved with a bias voltage.^{17,18} A large charging energy provides even the key ingredient for identifying nonlocal Andreev transport in one of the schemes we propose.

Andreev reflection through quantum dots, a problem which combines Coulomb interaction, superconducting correlations, and nonequilibrium, has been extensively studied theoretically.^{17–24} Here, we apply the diagrammatic real-time transport theory of Ref. 17 and 18. The relevance from the experimental point of view is proven by the recent success in coupling superconductors to quantum dots in either a carbon nanotube^{25–28} or a semiconductor nanowire.^{29–31} In particular, we propose to investigate nonlocal effects in Andreev transport through a single-level quantum dot with one superconducting and two normal-conducting leads, which may be (i) ferromagnetic with collinear magnetization or (ii) non-

magnetic (see Fig. 1). Thereby we identify nonlocality either (i) by the dependence of the Andreev current on the relative orientation of the two ferromagnets that are biased with the same voltage or (ii) by the response of the current in one normal lead to the applied voltage in the other one.

II. MODEL

The Hamiltonian of the system is $H = H_{\text{dot}} + \sum_{\eta} (H_{\eta} + H_{\text{tunn},\eta})$. The label $\eta = L, R, S$ corresponds to the left, right, and the superconducting lead, respectively. The dot is described by the Anderson-impurity model

$$H_{\text{dot}} = \sum_{\sigma} \epsilon d_{\sigma}^{\dagger} d_{\sigma} + U n_{\uparrow} n_{\downarrow}, \quad (1)$$

where $d_{\sigma}^{(\dagger)}$ is the annihilation (creation) operator for a dot electron with spin σ , $n_{\sigma} = d_{\sigma}^{\dagger} d_{\sigma}$ is the corresponding number operator, ϵ the energy of the spin-degenerate single-particle level, and U the on-site Coulomb repulsion. The Hamiltonian of the lead η reads

$$H_{\eta} = \sum_{k\sigma} \epsilon_{\eta k\sigma} c_{\eta k\sigma}^{\dagger} c_{\eta k\sigma} - g_{\eta} \sum_{k,k'} c_{\eta k\uparrow}^{\dagger} c_{\eta-k\downarrow}^{\dagger} c_{\eta-k'\downarrow} c_{\eta k'\uparrow}, \quad (2)$$

where the single-particle energies $\epsilon_{\eta k\sigma}$ are spin dependent in the case of ferromagnetic leads (with the quantization axis for σ being along the magnetization direction of the left lead) and the BCS pairing-interaction strength g_{η} is nonvanishing

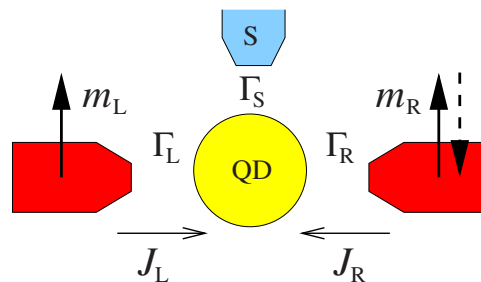


FIG. 1. (Color online) Setup: a quantum dot is tunnel coupled to one superconducting and two normal-conducting leads. The latter may be ferromagnetic with magnetization directions $\hat{\mathbf{m}}_L$ and $\hat{\mathbf{m}}_R = \pm \hat{\mathbf{m}}_L$.

only for $\eta=S$. The lead-electron operators are $c_{\eta k\sigma}$ and $c_{\eta k\sigma}^\dagger$. We treat the superconductor on a mean-field level, which introduces the notion of fermionic quasiparticles and a Cooper-pair condensate. The coupling between the dot and the leads is taken into account by the tunneling Hamiltonians

$$H_{\text{tunn},\eta} = V_\eta \sum_{k\sigma} (c_{\eta k\sigma}^\dagger d_\sigma + \text{H.c.}), \quad (3)$$

where for simplicity the tunnel matrix elements V_η are considered to be spin and wave vector independent.

The spin-resolved tunnel-coupling strengths are defined as $\Gamma_{\eta\sigma} = 2\pi |V_\eta|^2 \sum_k \delta(\omega - \epsilon_{k\sigma}) = 2\pi |V_\eta|^2 \rho_{\eta\sigma}$, with $\rho_{\eta\sigma}$ being the density of states of the spin species σ in lead η , which we assume to be constant. We also define the mean level broadening $\Gamma_\eta = \frac{1}{2} \sum_\sigma \Gamma_{\eta\sigma}$. The spin polarization of lead η is defined as $p_\eta = (\rho_{\eta+} - \rho_{\eta-}) / (\rho_{\eta+} + \rho_{\eta-})$, with $+$ ($-$) denoting the majority (minority) spins.

III. METHOD

We integrate out the leads' degrees of freedom to obtain an effective description of the quantum dot, whose Hilbert space is spanned by the four basis states $|\chi\rangle \in \{|0\rangle, |\uparrow\rangle, |\downarrow\rangle, |D\rangle \equiv d_\uparrow^\dagger d_\downarrow^\dagger |0\rangle\}$, with energies E_0 , $E_\uparrow = E_\downarrow$, and E_D corresponding to an empty, singly, and doubly occupied dot. It is useful to define the detuning $\delta = E_D - E_0 = 2\epsilon + U$. The dot is described by its reduced density matrix, ρ_{red} , whose matrix elements are $P_{\chi_2}^{\chi_1} \equiv \langle \chi_1 | \rho_{\text{red}} | \chi_2 \rangle$. The superconducting proximity effect induces a finite pair amplitude on the dot, expressed by the off-diagonal matrix element $P_D^0 = (P_D^0)^*$.

In the stationary limit, the elements of the reduced density matrix obey the generalized master equation

$$i(E_{\chi_1} - E_{\chi_2}) P_{\chi_2}^{\chi_1} = \sum_{\chi'_1 \chi'_2} W_{\chi_2 \chi'_2}^{\chi_1 \chi'_1} P_{\chi'_2}^{\chi'_1}, \quad (4)$$

with generalized rates $W_{\chi_2 \chi'_2}^{\chi_1 \chi'_1}$ that can be computed by means of a real-time diagrammatic technique.^{17,18,32–35} The stationary current out of lead η can be expressed as

$$J_\eta = -\frac{e}{\hbar} \sum_{\chi \chi'_1 \chi'_2} W_{\chi \chi'_2}^{\chi'_1 \eta} P_{\chi'_2}^{\chi'_1}, \quad (5)$$

where $W_{\chi \chi'_2}^{\chi'_1 \eta} \equiv \sum_s W_{\chi \chi'_2}^{\chi'_1 s \eta}$ and $W_{\chi \chi'_2}^{\chi'_1 s \eta}$ is the sum of all generalized rates that describe transitions in which in total s electrons are removed from lead η .

The diagrammatic rules to compute the diagrams contributing to the rates in the presence of superconducting leads are given in Ref. 18, those for diagrams in the presence of ferromagnetic leads are given in Refs. 34 and 35. In the following, we assume small and equal tunnel-coupling strengths $\Gamma_L = \Gamma_R \equiv \Gamma_N < T$ to the left and right leads, which we keep up to first order in the calculation of the current. The chemical potential of the superconductor is chosen as the reference for the energies, i.e., $\mu_S = 0$. To study subgap transport, we consider the limit of a large superconducting order parameter $\Delta \rightarrow \infty$, which we choose to be real. In this case,

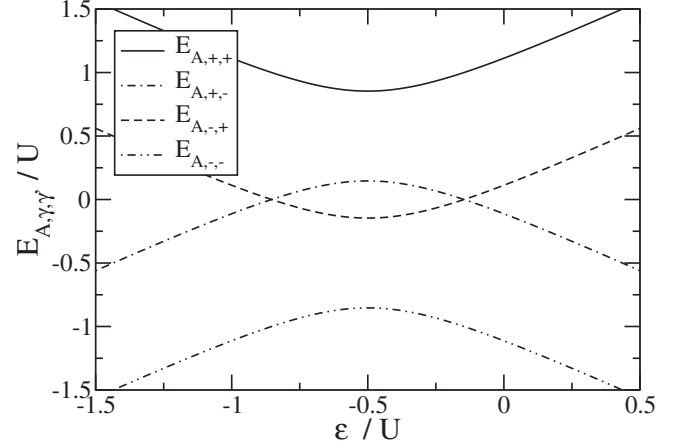


FIG. 2. Andreev bound-state energies as a function of the level position ϵ , with $\Gamma_S/U=0.2$ and $\Gamma_N=0$.

all orders in the tunnel-coupling strength with the superconductor Γ_S can be resummed exactly.^{18,36} In the absence of a superconducting lead, the excitation energies of the dot, ϵ and $\epsilon+U$, are split by the charging energy U . Due to the tunnel coupling to a superconductor the particle and hole sector of the Hilbert space are mixed, leading to four Andreev bound-state energies, defined as poles of the retarded Green's function of the dot for $\Gamma_N=0$,

$$E_{A,\gamma',\gamma} = \gamma' \frac{U}{2} + \gamma \sqrt{\left(\epsilon + \frac{U}{2}\right)^2 + \frac{\Gamma_S^2}{4}}, \quad (6)$$

with $\gamma', \gamma = \pm 1$ (see Fig. 2). In the following, we also make use of the definition $\epsilon_A \equiv \sqrt{\left(\epsilon + \frac{U}{2}\right)^2 + \frac{\Gamma_S^2}{4}}$. The Andreev transport is largest for small detuning $|\delta|$. We consider the regime $|\delta| < \sqrt{U^2 - \Gamma_S^2}$, for which the inequality $E_{A,+,+} > E_{A,+,-} > 0 > E_{A,-,+} > E_{A,-,-}$ holds.

The Andreev channel supporting transport from a normal lead to a superconductor through a quantum dot can be switched between different states by an applied bias voltage μ_N .¹⁸ In the following we consider $\mu_N > 0$ (the case $\mu_N < 0$ is obtained from the symmetry transformation $\mu_N \rightarrow -\mu_N$, $\delta \rightarrow -\delta$, and $J_N \rightarrow -J_N$). The different states are characterized by how they influence and probe the state of the quantum dot.

For small bias voltage, $E_{A,+,-} > \mu_N$, all rates (to first order in Γ_N) involving an electron transfer from or to the normal lead are not affected by the superconductor. The current can be written in the simple form $J_N = \frac{2e}{\hbar} \Gamma_N (1 + Q/e)$, independent of the pair amplitude P_D^0 , where $Q/(-e) = \langle \sum_\sigma d_\sigma^\dagger d_\sigma \rangle = P_\uparrow + P_\downarrow + 2P_D$ (with $-2e \leq Q \leq 0$) is the average quantum-dot charge. The latter can be affected by the proximity effect in the quantum dot. In the stationary limit, the dot is singly occupied, $Q = -e$, and the Andreev channel is Coulomb blocked, $J_N = 0$. A current can only flow for $Q \neq -e$, which, e.g., could be achieved by attaching a voltage-biased third lead. For large bias voltage, $\mu_N > E_{A,+,+}$, the Andreev channel is also independent of the dot pair amplitude, with $J_N = \frac{2e}{\hbar} \Gamma_N (1 + Q/2e)$. In both cases, the subgap transport involves Andreev processes at the interface between quantum dot and the superconducting lead only. As a consequence, the

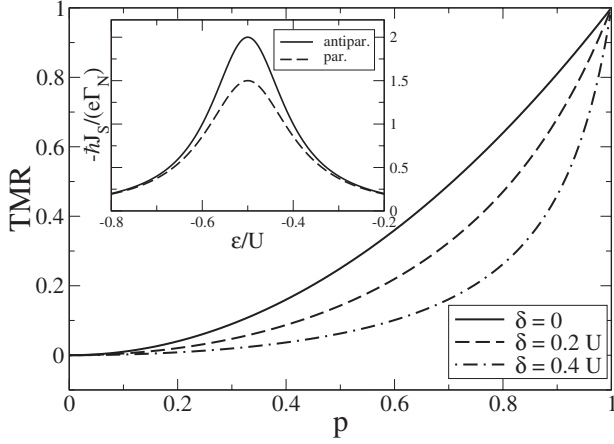


FIG. 3. TMR as a function of the polarization p for different values of the detuning $\delta=2\epsilon+U$. Inset: Current J_S in the superconducting lead as a function of ϵ , for polarization $p=0.5$ and parallel and antiparallel alignments of the leads' magnetization. For both graphs, we chose $\mu_L=\mu_R=\mu_N=U$, $\mu_S=0$, $\Gamma_S=0.2U$, $\Gamma_L=\Gamma_R=0.001U$, and $k_B T=0.01U$.

current is, in both cases, insensitive to the sign of the detuning δ . This is different for the regime of intermediate voltages, $E_{A,+} > \mu_N > E_{A,-}$. In this case the rates involving an electron transfer to or from the normal lead do depend on δ and Γ_S , the rates $W_{0\sigma}^{D\sigma}$ and $W_{D\sigma}^{0\sigma}$ describing proximization of the quantum dot are nonvanishing, and the current in the normal lead also depends on the pair amplitude P_0^D . An interesting feature of this regime is that a positive detuning drives the dot to an average occupation of less than one electron, thus overcompensating the effect of the finite bias voltage.¹⁸

IV. CROSSED ANDREEV REFLECTION

We first consider the case of ferromagnetic leads with equal polarization strengths $|p_L|=|p_R|=p$ kept at the same chemical potential μ_N and characterized by the same Fermi distribution $f_N(\epsilon)=[1+\exp(\epsilon-\mu_N)/k_B T]^{-1}$. Crossed Andreev transport is identified by its dependence on the relative orientation of the ferromagnets, quantified by the tunneling magnetoresistance (TMR) $\text{TMR} \equiv (J_S^{\text{AP}} - J_S^{\text{P}})/J_S^{\text{AP}}$, where $J_S^{\text{P(} \overline{\text{AP}} \text{)}} = (2e\Gamma_S/\hbar)\text{Im} P_0^D$ is the current in the superconductor for parallel (antiparallel) alignment of the magnetizations. The stationary pair amplitude $P_0^D = \langle d_\downarrow d_\uparrow \rangle$, in zeroth order in Γ_N and in the $\Delta \rightarrow \infty$ limit, is calculated from the equation $P_0^D = \sum_\chi W_{0\chi}^{D\chi} P_\chi^D / [W_{00}^{DD} - i(2\epsilon + U)]$. In the inset of Fig. 3 we show the current in the superconducting lead for both the parallel and antiparallel alignments of the magnetizations as a function of the gate voltage for $\mu_N=U$ (large-bias regime). The current shows a peak around zero detuning, $\epsilon=-U/2$, with a width given by Γ_S . The subgap current for the parallel alignment is clearly suppressed, indicating the presence of CAR. The TMR is plotted in Fig. 3 as a function of the polarization strength p for different values of the detuning δ . For small values of p the TMR exhibits a quadratic dependence on p ,

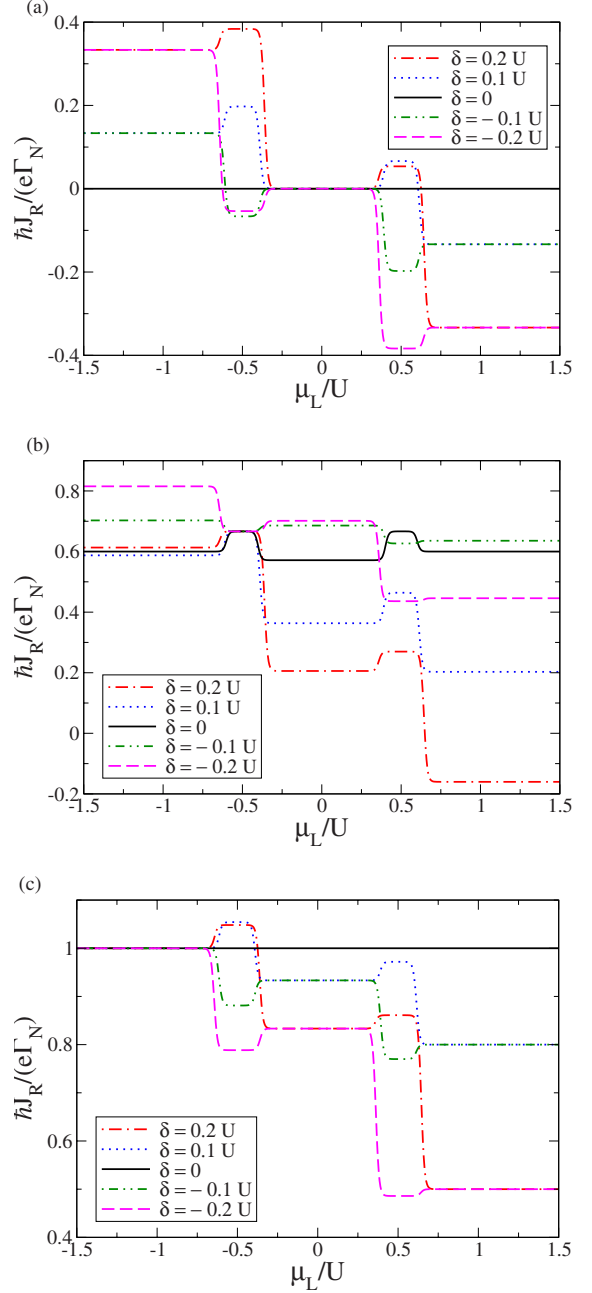


FIG. 4. (Color online) Current J_R in the right lead as a function of the chemical potential μ_L of the left lead for different values of the detuning δ and $\Gamma_S=0.2U$, $\Gamma_L=\Gamma_R=0.001U$, $p_L=p_R=0$, $k_B T=0.01U$, and (a) $\mu_R=0$ (small bias), (b) $\mu_R=0.5U$ (intermediate bias), and (c) $\mu_R=U$ (large bias).

$$\text{TMR} \approx \frac{\left\{ 1 - \Pi_{\gamma=\pm} \left[\sum_{\gamma'=\pm} \gamma' f_N(E_{A,\gamma',\gamma}) \right] \right\} \Gamma_S^2 p^2}{4\epsilon_A^2 - \left[\sum_{\gamma,\gamma'=\pm} \gamma\gamma' \left(\epsilon + \frac{U}{2} + \epsilon_A \right) f_N(E_{A,\gamma',\gamma}) \right]^2}, \quad (7)$$

which simplifies in the regime of large bias voltage to $\text{TMR} \approx p^2$ for $|\delta| \ll \Gamma_S$ and $\text{TMR} \approx p^2 \Gamma_S^2 / \delta^2$ for $|\delta| \gg \Gamma_S$, and in the regime of intermediate (positive) bias voltage to

$\text{TMR} \approx 4p^2/3$ for $|\delta| \ll \Gamma_S$, $\text{TMR} \approx p^2\Gamma_S^2/\delta^2$ for $-\delta \gg \Gamma_S$, and $\text{TMR} \approx 2p^2$ for $\delta \gg \Gamma_S$.

V. NEGATIVE NONLOCAL CONDUCTANCE

We now look for nonlocal effects in Andreev transport for nonmagnetic leads, $p_L=p_R=0$, by studying the current in the right lead, J_R , as a function of the voltage applied to the left lead μ_L . For a three-terminal device, we define a nonlocal conductance, $G^{\text{nl}} \equiv J_R/(\mu_S - \mu_L)$, as the current response in the right lead to a voltage bias between superconductor and left lead. In particular, we will consider the nonlocal differential conductance $G_{\text{diff}}^{\text{nl}} \equiv -\partial J_R/\partial \mu_L$. Direct transport between the two normal leads contributes with a positive sign to $G_{\text{diff}}^{\text{nl}}$. Nonlocal transport channels such as CAR may contribute with a negative sign. For a large class of such three-terminal devices, however, it has been shown³⁷ that the sum of all contributions to $G_{\text{diff}}^{\text{nl}}$ remains positive. In contrast, we find for our system regimes with negative values of $G_{\text{diff}}^{\text{nl}}$ and, even more striking, negative values of G^{nl} .

In Figs. 4(a)–4(c), we show the current in the right lead as a function of the electrochemical potential in the left lead for the three cases of a small, intermediate, and large voltage μ_R applied to the current probe, respectively. Several features of these current-voltage characteristics indicate the strong coupling of the quantum dot to a superconducting lead. First, there are four steps (instead of two) associated with the four Andreev bound-state energies. Second, the height of many of the plateaus is sensitive to the detuning δ . In the cases displayed in Figs. 4(a) and 4(c), the plateau height of the current, given by $J_R=2e\Gamma_N(1+Q/e)$ and $J_R=2e\Gamma_N(1+Q/2e)$, respectively, directly reflects the average quantum-dot charge, which is strongly influenced by the proximity effect.^{18,38} For $\delta=0$, the proximity effect is maximal, with $Q=-e$ for all values of the bias voltages, which leads to $J_R=0$ and $J_R=e\Gamma_N$ in Figs. 4(a) and 4(c), respectively. With increasing $|\delta|$, the proximity effect decreases and the current approaches the value expected in the absence of the superconducting lead. Third, the striking feature indicating nonlocal Andreev transport is the nonmonotonic dependence of J_R on μ_L , i.e., the appearance of a negative nonlocal differential conductance, $G_{\text{diff}}^{\text{nl}} < 0$. Even more remarkable is for $\mu_R=0$ the negative nonlocal conductance $G^{\text{nl}} < 0$ that occurs for positive/negative detuning δ at positive/negative μ_L in the intermediate-bias regime. To understand this behavior, we realize that in this regime there are combined Andreev processes that involve both the interfaces from the quantum dot to the superconductor and the left lead, while there are no Andreev processes involving electron transfer between quantum dot and right lead. The intermediate-voltage Andreev transport between left lead and superconductor yields an av-

erage dot charge that is determined by the dot level's position relative to the chemical potential of the superconductor rather than that of the normal lead: for positive (negative) detuning the probability of double occupation decreases (increases) and the average occupation of the dot is smaller (larger) than one. This deviation from single occupancy is probed by the right lead. Changing the sign of detuning leads to a sign change in the current measured in the right lead.

We remark that the negative nonlocal conductance is not due to CAR. In fact, making the normal-conducting leads ferromagnetic suppresses the negative nonlocal conductance, independent of whether the ferromagnets are aligned parallel or antiparallel, since a finite spin accumulation on the quantum dot reduces the dot pair amplitude. For CAR an enhanced (reduced) effect would be expected for the antiparallel (parallel) alignment. The effect that we predict is rather a consequence of combined Andreev processes between left lead and superconductor. The negative nonlocal conductance can only be probed because of a large charging energy that prohibits direct transport between the normal-conducting leads.

VI. CONCLUSIONS

We investigated nonlocal Andreev transport through an interacting quantum dot in a three-terminal setup with one superconducting and two normal-conducting leads. We considered two different biasing schemes. In the first one, the normal-conducting leads are ferromagnetic with collinear magnetizations and they are kept at the same chemical potential. The key result for this case is that CAR occurs due to the nonequilibrium proximity effect in the dot and it is characterized by a finite TMR. In the second scheme, the two normal-conducting leads are nonmagnetic and the response of the current in one lead to the voltage applied to the other one is studied. In that case, nonlocal Andreev transport is identified by negative values of the nonlocal differential conductance. Even more strikingly, we find regimes with negative values of the full nonlocal conductance. The virtue of employing quantum dots lies, first, in the possibility to tune the Andreev channels by a gate voltage and, second, in the presence of a large charging energy which generates specific transport regimes characterized by a negative nonlocal conductance. Both aspects are advantageous for a clear identification of nonlocal Andreev transport.

ACKNOWLEDGMENTS

We acknowledge useful discussions with W. Belzig, M. Eschrig, and A. Zaikin and financial support from DFG via Project No. SFB 491.

- ¹A. F. Andreev, *Sov. Phys. JETP* **19**, 1228 (1964).
- ²G. Falci, D. Feinberg, and F. W. J. Hekking, *Europhys. Lett.* **54**, 255 (2001).
- ³G. B. Lesovik, T. Martin, and G. Blatter, *Eur. Phys. J. B* **24**, 287 (2001).
- ⁴T. Yamashita, S. Takahashi, and S. Maekawa, *Phys. Rev. B* **68**, 174504 (2003).
- ⁵D. Sánchez, R. López, P. Samuelsson, and M. Büttiker, *Phys. Rev. B* **68**, 214501 (2003).
- ⁶R. Mélin and D. Feinberg, *Phys. Rev. B* **70**, 174509 (2004).
- ⁷J. P. Morten, A. Brataas, and W. Belzig, *Phys. Rev. B* **74**, 214510 (2006).
- ⁸A. Brinkman and A. A. Golubov, *Phys. Rev. B* **74**, 214512 (2006).
- ⁹M. S. Kalenkov and A. D. Zaikin, *Phys. Rev. B* **75**, 172503 (2007).
- ¹⁰D. S. Golubev and A. D. Zaikin, *Phys. Rev. B* **76**, 184510 (2007).
- ¹¹M. S. Kalenkov and A. D. Zaikin, *Phys. Rev. B* **76**, 224506 (2007).
- ¹²S. I. Bozhko, V. S. Tsoi, and E. Yakolev, *JETP Lett.* **36**, 153 (1982).
- ¹³P. A. M. Benistant, H. van Kempen, and P. Wyder, *Phys. Rev. Lett.* **51**, 817 (1983).
- ¹⁴D. Beckmann, H. B. Weber, and H. v. Löhneysen, *Phys. Rev. Lett.* **93**, 197003 (2004).
- ¹⁵S. Russo, M. Kroug, T. M. Klapwijk, and A. F. Morpurgo, *Phys. Rev. Lett.* **95**, 027002 (2005).
- ¹⁶P. Cadden-Zimansky and V. Chandrasekhar, *Phys. Rev. Lett.* **97**, 237003 (2006).
- ¹⁷M. G. Pala, M. Governale, and J. König, *New J. Phys.* **9**, 278 (2007).
- ¹⁸M. Governale, M. G. Pala, and J. König, *Phys. Rev. B* **77**, 134513 (2008).
- ¹⁹R. Fazio and R. Raimondi, *Phys. Rev. Lett.* **80**, 2913 (1998).
- ²⁰R. Fazio and R. Raimondi, *Phys. Rev. Lett.* **82**, 4950 (1999).
- ²¹K. Kang, *Phys. Rev. B* **58**, 9641 (1998).
- ²²P. Schwab and R. Raimondi, *Phys. Rev. B* **59**, 1637 (1999).
- ²³A. A. Clerk, V. Ambegaokar, and S. Hershfield, *Phys. Rev. B* **61**, 3555 (2000).
- ²⁴J. C. Cuevas, A. Levy Yeyati, and A. Martín-Rodero, *Phys. Rev. B* **63**, 094515 (2001).
- ²⁵M. R. Buitelaar, T. Nussbaumer, and C. Schönenberger, *Phys. Rev. Lett.* **89**, 256801 (2002).
- ²⁶J.-P. Cleuziou, W. Wernsdorfer, V. Bouchiat, T. Ondarçuhu, and M. Monthieux, *Nat. Nanotechnol.* **1**, 53 (2006).
- ²⁷P. Jarillo-Herrero, J. A. van Dam, and L. P. Kouwenhoven, *Nature (London)* **439**, 953 (2006).
- ²⁸H. I. Jørgensen, K. Grove-Rasmussen, T. Novotný, K. Flensberg, and P. E. Lindelof, *Phys. Rev. Lett.* **96**, 207003 (2006).
- ²⁹J. A. van Dam, Y. V. Nazarov, E. P. A. M. Bakkers, S. De Franceschi, and L. P. Kouwenhoven, *Nature (London)* **442**, 667 (2006).
- ³⁰T. Sand-Jespersen, J. Paaske, B. M. Andersen, K. Grove-Rasmussen, H. I. Jørgensen, M. Aagesen, C. B. Sørensen, P. E. Lindelof, K. Flensberg, and J. Nygård., *Phys. Rev. Lett.* **99**, 126603 (2007).
- ³¹C. Buizert, A. Oiwa, K. Shibata, K. Hirakawa, and S. Tarucha, *Phys. Rev. Lett.* **99**, 136806 (2007).
- ³²J. König, H. Schoeller, and G. Schön, *Phys. Rev. Lett.* **76**, 1715 (1996).
- ³³J. König, J. Schmid, H. Schoeller, and G. Schön, *Phys. Rev. B* **54**, 16820 (1996).
- ³⁴J. König and J. Martinek, *Phys. Rev. Lett.* **90**, 166602 (2003).
- ³⁵M. Braun, J. König, and J. Martinek, *Phys. Rev. B* **70**, 195345 (2004).
- ³⁶A. V. Rozhkov and D. P. Arovas, *Phys. Rev. B* **62**, 6687 (2000).
- ³⁷J. P. Morten, A. Brataas, and W. Belzig, *Appl. Phys. A* **89**, 609 (2007).
- ³⁸I. A. Sadovskyy, G. B. Lesovik, and G. Blatter, *Phys. Rev. B* **75**, 195334 (2007).